HHS Public Access

Author manuscript

Am J Med Genet A. Author manuscript; available in PMC 2023 January 01.

Published in final edited form as:

Am J Med Genet A. 2022 January ; 188(1): 104–115. doi:10.1002/ajmg.a.62497.

Genetic and Phenotypic Heterogeneity in KIAA0753-related Ciliopathies

Katherine A. Inskeep[1], **Yuri A. Zarate**[2], **Danielle Monteil, CDR, MC, USN**[3], **Jurgen Spranger**[4], **Dan Doherty**[5], **Rolf W. Stottmann**[1,6,7,*], **K. Nicole Weaver**[6,7,*]

[1]Division of Developmental Biology, Cincinnati Children's Hospital Medical Center, Cincinnati, OH

[2]Section of Genetics and Metabolism, University of Arkansas for Medical Sciences, Little Rock, AR

[3]Department of Pediatrics, Naval Medical Center Portsmouth, Portsmouth, VA.

[4]Children's Hospital, University of Mainz/Germany

[5]University of Washington, Seattle, WA

[6]Division of Human Genetics, Cincinnati Children's Hospital Medical Center, Cincinnati, OH

[7]Department of Pediatrics, University of Cincinnati College of Medicine, Cincinnati, OH

Abstract

Primary ciliopathies are heterogenous disorders resulting from perturbations in primary cilia form and/or function. Primary cilia are cellular organelles which mediates key signaling pathways during development, including in the brain. The Sonic hedgehog (Shh) pathway is mediated by primary cilia and required for neuroepithelium and central nervous system development. The proteins which transduce Shh signaling are located within the primary cilia. Joubert syndrome is a primary ciliopathy characterized by cerebellar/brain stem malformation, hypotonia, and developmental delays. Variants in more than 35 genes are associated with Joubert syndrome, including the gene *KIAA0753*. KIAA0753 is localized at the basal body/centrosome and is part of a complex required for primary ciliogenesis. The phenotypic spectrum of human patients with biallelic pathogenic variants in *KIAA0753* (OMIM 617127) is broad and not well-characterized. Here we describe four individuals with biallelic pathogenic *KIAA0753* variants, including 5 novel variants. We report *in vitro* results assessing the function of each variant indicating that KIAA0753 protein is produced, but is not fully competent to promote primary ciliogenesis. Ablation of KIAA0753 *in vitro* blocks primary ciliogenesis and Shh pathway activity. Correspondingly, *KIAA0753* patient fibroblasts have a deficit in primary ciliation and improper Shh and Wnt signaling, with a particularly blunted response to Shh pathway stimulation. Our work expands the

Correspondence to: Nicole Weaver, MD, 513 636 7294 (fax), 513 803 7431 (phone), Kathryn.weaver@cchmc.org.
*These authors contributed equally

Conflict of interest Statement: The authors have no conflicts of interest to declare.

phenotypic spectrum of KIAA0753 ciliopathies. We also demonstrate the utility of patient-focused functional assays for proving causality of genetic variants and understanding the relationship between variants and phenotypes as part of the ongoing effort to definitively categorize variants of unknown significance.

Introduction

Primary cilia are dynamic, microtubule based organelles which extend from almost every cell type and play an essential role in regulating many crucial molecular signaling pathways(1). Ciliopathies are disorders associated with perturbations in the structure and/or function of the primary cilium. Ciliopathies are associated with a broad phenotypic spectrum which can include congenital structural anomalies in nearly every organ system as well as progressive phenotypes such as obesity and retinal degeneration – ref?. There are at least 35 genes in which pathogenic variants cause ciliopathy syndromes(2). Joubert syndrome (JS), orofacial digital syndrome (OFD), and Meckel syndrome (MKS) are clinically defined disease categories with an overlap in phenotypic features and genetic etiologies. Joubert syndrome is characterized by the triad of the “molar tooth sign” (a characteristic cerebellar/brain stem malformation seen on brain imaging), hypotonia, and developmental delays. Orofacial digital syndrome is associated with hypertelorism, digital abnormalities, and intra-oral abnormalities such as cleft palate and tongue lobulations. Meckel syndrome is classically defined as the triad of cystic kidneys, occipital encephalocele, and hepatic fibrosis. Short-rib ±polydactyly syndrome (SRPS), is associated with short long bones, narrow chest, with or without polydactyly. While each of these 4 syndromes has pathognomonic associated features, they are all caused by pathogenic variants in genes involved in ciliary function or structure. With expanding access to broad next-generation sequencing, it has been increasingly recognized that ciliopathy phenotypes are often a continuum between JS, MKS, SRPS, and OFD (and others), rather than discrete syndromes. For example, molar tooth sign has been described in individuals with OFD syndrome, and liver and kidney cysts can be associated with JS.

KIAA0753 (also known as moonraker and OFIP) is a centrosome and pericentriolar satellite protein implicated in cilia formation as well as centriolar duplication and microtubule stability (3, 4). Biallelic pathogenic variants in *KIAA0753* were first associated with human phenotypes in 2016, when 1 patient was reported with OFD syndrome accompanied by a molar tooth sign (3). To date, there have been 8 patients with biallelic pathogenic variants in *KIAA0753* reported in the literature(5–8): two are described as having JS, one with OFD, and six with SRPS (Table 1). The majority of reported *KIAA0753* variants predict premature truncation of the KIAA0753 protein. KIAA0753 is required for the formation of a trimeric complex with OFD1 (the genetic cause of OFD syndrome type I) and centrosomal protein 20 (FOPNL), which is essential for basal body anchoring and cilia formation (9–11). Chevrier et al (2016) demonstrated that C-terminal truncated KIAA0753 protein is unable to interact with OFD1 and FOPN(3). Stephen et al (2017) studied fibroblasts from siblings who were compound heterozygous for splice site and missense variants in *KIAA0753*, and showed a lower percentage of ciliated cells with no difference in cilia length in patients versus controls after serum starvation(7).

We report 4 new patients with 6 biallelic pathogenic variants in *KIAA0753* (5 novel variants). In contrast to previously reported patients, all 4 were diagnosed prenatally with structural abnormalities. Based upon the established role of KIAA0753, we hypothesized that these variants would lead to a significant defect in primary ciliogenesis. Further, as cilia are known to play essential roles in the transduction of Wnt and Sonic hedgehog (Shh) signaling, proper spatiotemporal expression of these essential molecular signals is required for normal development(12). However, the effect of disrupted KIAA0753 function on the Wnt and Shh pathways has not previously been studied. We hypothesized that loss of functional KIAA0753 would be sufficient to disrupt these cellular signaling pathways *in vitro*. We demonstrate the utility of *in vitro* experimental methods to support pathogenicity, determine the effects of patient variants on cellular signaling, and explore the effects on Wnt and Shh signaling in patient fibroblasts.

Results

Clinical Description of 4 Individuals with Biallelic variants in *KIAA0753*

Patient 1 is a 4.5-year-old male who was diagnosed prenatally with ventriculomegaly, vermian hypoplasia, and Dandy-Walker malformation (Fig.1 A–C). He was born at 37 weeks gestation. Birth length was 50.5 cm (62nd centile), weight was 2.8 kg (10th centile), and head circumference was 38.5 cm (99th centile). After birth, he was admitted to the neonatal intensive care unit (NICU) for management of apnea and poor feeding. Brain magnetic resonance imaging (MRI) after birth demonstrated a molar tooth sign, vermian hypoplasia, and polymicrogyria. Physical exam was notable for frontal bossing, flat nasal bridge, hypertelorism, a short, upturned nose, and bilateral post-axial polydactyly. Clinical exome sequencing in infancy was non-diagnostic. Targeted exome reanalysis upon the birth of a sibling (Patient 2) with similar physical features identified biallelic likely pathogenic variants in *KIAA0753* (c.2803_2806dup/c.2825T>G; p.Asp936fs*3/p.Val942Gly). Currently, Patient 1 has a tracheostomy and is ventilator dependent, fed via gastrostomy tube, and noted to have significant global developmental delay. At age 4.5 years, length is 97.5 cm (1.6th centile), weight is 16.3 kg (26th centile), and head circumference is 57.5 cm (>99th centile). He is able to briefly sit unsupported and can stand with support. He vocalizes and is able to indicate preferences using an assistive communication device. He has non-epileptic body stiffening spells treated with gabapentin and clonazepam. Recent abdominal and renal ultrasounds identified no abnormalities. Dilated eye exam at age 4 years 3 months was significant only for congenital nystagmus and mild myopic astigmatism bilaterally.

Patient 2 is the brother of Patient 1. He was diagnosed prenatally with structural brain anomalies (ventriculomegaly, Dandy-Walker variant, Fig.1 D–F). He was born at 37 weeks gestation, required hospitalization in the NICU for 4 months, and ultimately was discharged with a tracheostomy and ventilator due to central apnea and gastrostomy tube for feeding. Post-natal MRI demonstrated bilateral perisylvian polymicrogyria, pontine hypoplasia, abnormal elongation of the superior cerebellar peduncles in molar tooth configuration, severe vermian hypoplasia, vermian dysplasia, asymmetric brain stem with right side smaller than left. There was concern for ectopic neurohypophysis. Echocardiogram in infancy was

notable only for a patent foramen ovale. His most recent growth parameters at age 23 months are weight 10 kg (6th centile), length 82 cm (6th centile), and head circumference 51 cm (98th centile). Facial features are similar to his brother, with hypertelorism, frontal bossing, and macrocephaly. He has truncal hypotonia and is able to hold his head up briefly. He is able to reach for objects and can roll but is not able to sit independently. He can imitate some gestures and makes vocalizations. His most recent renal ultrasound at age 22 months demonstrated normal kidneys. He has had breath-holding spells since birth which are treated with gabapentin. At 14 months he was started on levothyroxine for hypothyroidism. Growth hormone stimulation and ACTH stimulation testing were normal. Dilated eye exam at age 21 months was significant for intermittent esotropia and bilateral hyperopia, which was first identified at 1 year of age and for which he wears full time glasses with full correction (began wearing at age 1). Abdominal ultrasound at age 22 months identified a small accessory spleen in the splenic hilum; no hepatic cysts.

Patient 3 was diagnosed prenatally with growth retardation and ventriculomegaly, cerebellar hypoplasia, and enlarged cisterna magna (Fig.1 G,H). All bones in his extremities measured less than 1st centile and distal bowing of the arms was noted. Amniocentesis was performed to assess karyotype which was normal (46, XY). A skeletal dysplasia sequencing panel (GeneDx) was ordered which identified a variant of uncertain significance in *RUNX2* (c.243_260del18; p.Ala84_Ala89del) inherited from his phenotypically normal father. A fetal echocardiogram was also performed and was normal. He was born at 33 weeks 2 days gestation via Caesarean section for non-reassuring fetal heart tones. Birth weight and length were within normal limits (2.34 kg, 74th centile; 43 cm, 38th centile). He had macrocephaly (head circumference 37 cm, > 2 SD). He was admitted to the NICU for management of pulmonary hypoplasia and pulmonary hypertension. Physical exam was notable for frontal bossing, low-set ears, anteverted nares, and macrocephaly. He had a narrow chest, short limbs, brachydactyly, penoscrotal hypospadias and cryptorchidism. Plain films demonstrated skeletal abnormalities including short ribs, trident ilia, broad metaphyses, short and bowed tubular bones, and short metacarpals. He died at 2 weeks of age due to severe pulmonary hypertension. Rapid whole exome sequencing (GeneDx) identified biallelic truncating variants in *KIAA0753* (c.943C>T/c.2656C>T; p. Gln315*/p.R886*).

Patient 4 was twin B of a pregnancy conceived via intracytoplasmic sperm injection. An ultrasound at approximately 19 weeks gestation raised concerns about macrocephaly with biparietal diameter and head circumference, which were approximately 2 weeks ahead of other growth parameters. Intracranial findings included ventriculomegaly with enlarged third and lateral ventricles, Dandy-Walker malformation, and absent cavum septum pellucidum raising concern for agenesis of the corpus callosum. Postaxial polydactyly of one hand was also noted. The ultrasound confirmed dichorionic diamniotic twins with adequate amniotic fluid volume. A fetal echocardiogram was performed and noted a VSD in Twin B.

Fetal MRI revealed a large head with hypertelorism, mild ventriculomegaly, complete agenesis of the corpus callosum, normal third ventricle, dilated fourth ventricle with dysplasia of the cerebellar vermis, and interdigitation of the cortex with abnormally folded medial cortex bilaterally raising concern for cortical dysplasia (Fig.1 I,J,). The brainstem was judged to be abnormal with a dorsal mass at the cervicomedullary junction,

the cerebellar vermis small and upwardly rotated, and the superior cerebellar peduncles thickened and horizontally oriented. In addition, a small defect in the foramen magnum at the base of the skull was noted. Selective termination of twin B was performed. Post mortem whole exome sequencing identified biallelic truncating variants in *KIAA0753* (c.1891A>T/ c.1571_1572delGA; p.Lys631*/ p.Arg524Thrfs*7).

In vitro analysis of novel *KIAA0753* variants

KIAA0753 patient variants result in stable, truncated proteins—We hypothesized that any of the five frameshift/early stop patient variants in this cohort (Fig. 2A) would truncate the translated KIAA0753 protein, which may impact its ability to facilitate primary ciliogenesis. The missense variant (V942G) is located in the C-terminal region of KIAA0753 which has been shown to be required for its interaction with OFD1 and FOPNL(3). Therefore, we hypothesized this missense variant would have a similar effect to the variants which truncate the C terminus. First, we asked whether the variant KIAA0753 sequences would produce stable proteins. Western immunoblotting of protein from transfected NIH3T3 cells showed expression of KIAA0753 at the expected molecular weight of 115 kDa in wild-type cells transfected with wild-type KIAA0753. Interestingly, by transfecting KIAA0753 patient variant plasmids into KIAA0753 KO cells, we find that all six variant transcripts are expressed, and their protein sizes correlate to their predicted molecular weights based upon the location of each truncating or missense variant. This indicates that KIAA0753 protein is produced, but it lacks the C-terminus in many of the predicted pathogenic variants.

KIAA0753 patient variants do not rescue defective ciliogenesis in KIAA0753-ablated cells—In order to study the ability of KIAA0753 variant proteins to function in ciliogenesis, we first ablated the *KIAA0753* gene *in vitro* and then overexpressed each variant sequence within a separate plasmid. CRISPR-Cas9 guides were designed to create a large deletion of *KIAA0753* in NIH3T3 cells. Sanger sequencing revealed one clonal line (KIAA0753 KO) with bi-allelic deletions causing frameshift stops in Exon 3 (Fig. 2A). We assessed primary cilia formation in this KIAA0753 KO line through immunocytochemistry of acetylated tubulin staining in serum-starved cells. We showed a total lack of primary cilia in KIAA0753 KO cells (Fig. 2B–D). We then asked whether primary ciliogenesis would be ‘rescued’ by transfection of full-length KIAA0753 plasmid. This is indeed the case as ciliation percentage increases from 4.4% to 28.5% when KIAA0753 KO cells are transfected with wild-type KIAA0753 plasmid. However, none of the six patient variants are able to significantly rescue primary ciliogenesis *in vitro* (Fig. 2G; ciliation ranges from 3.0%-7.8%).

Shh signaling is disrupted in KIAA0753 knock-out cells—Given the role of primary cilia in Shh signaling, we investigated whether Shh signaling was affected by loss of the cilia in KIAA0753 KO cells. We treated cells with Smoothened Agonist (SAG), which activates the Shh pathway via direct binding to Smoothened. RT-qPCR for the transcriptional target gene *Gli1* revealed that KIAA0753 KO cells do not upregulate *Gli1* in response to SAG, indicating that the Shh pathway is disrupted by lack of cilia in these cells (Fig 2E).

KIAA0753 patient fibroblasts lack primary cilia—Previous reports have shown that KIAA0753 localizes to the basal body of the primary cilia(3). We confirmed this in the NIH3T3 cells by staining for acetylated alpha-tubulin (ciliary axoneme) and gamma tubulin (basal body) in both mouse (NIH3T3, Fig. 3A–F) and human (Fig. 3G–J) fibroblasts. Primary fibroblasts obtained from Patient 1 were similarly analyzed. Compared to wild-type human primary fibroblasts which exhibit ~40% ciliation without stimulation and ~60% ciliation when serum starved, KIAA0753 patient fibroblasts are ~15% ciliated without stimulation and ~30% ciliated upon serum starvation, indicating a 50% reduction in primary cilia in patient cells (Fig. 3J–K).

KIAA0753 is required for Shh and Wnt signaling responses in patient cells—In order to perform an unbiased genome wide analysis of response to SHH and WNT pathway activation, we performed RNA sequencing on control and patient primary fibroblast cells, either untreated or stimulated with SAG or WNT3A conditioned media. All conditions were run with triplicate samples. We found that KIAA0753 patient cells have a generally blunted response to SAG stimulation, shown by a low number of differentially expressed genes between the untreated and treated patient samples, as well as minimal fold change in expression of any of the major Shh response genes (Fig. 4A and B, respectively). Treatment with WNT3A normally upregulates the Wnt pathway. We found in this case that while there are differentially expressed genes between WNT3A-treated and untreated samples, the WNT response factor *Axin2* is not upregulated as normal in patient cells, although *Dkk1*, another Wnt gene, is unchanged (Fig. 4C). We conclude from the RNA sequencing data that KIAA0753 is required for Shh signaling and some aspects of Wnt signaling.

Discussion

We report 4 new individuals with biallelic pathogenic variants in *KIAA0753* and phenotypes that exemplify the spectrum that can be seen in ciliopathy patients. *KIAA0753*-related syndrome spectrum is a phenotypic continuum from lethal skeletal dysplasia with JS features at the most severe end, through non-lethal metaphyseal skeletal dysplasia with short ribs and OFD, and JS only at the mildest end. *KIAA0753* represents another example of a single ciliopathy gene that can cause different clinical syndromes (3, 5, 7, 8).

Previous reports have shown that KIAA0753 is a necessary component of the basal body during primary ciliogenesis(3). Our *in vitro* assessment of six KIAA0753 variant proteins (1 missense, 5 frameshift/premature stop or nonsense) demonstrates that variant proteins are unable to rescue ciliogenesis in KIAA0753 KO NIH3T3 cells. This is consistent with previous reports of reduced cilia numbers in KIAA0753 patient fibroblasts. However, our results indicate that stable, truncated KIAA0753 protein is produced by each variant sequence and is not inherently unstable or targeted by the cell for degradation. Therefore, we suggest that the subsequent pathogenicity is due to loss of function which we suspect is further due to loss of the C-terminal region of the protein. However, we note that this overexpression experiment cannot rule out the possibility that endogenous KIAA0753 variant transcripts undergo nonsense mediated decay. Interestingly, there was no detectable difference in lack of rescue between the various premature truncation variants and the missense variant. This suggests that this particular missense variant also leads to a loss-of-

function effect. One important limitation to our work is that we examined each variant alone, rather than in compound heterozygous combinations as was found in the human patients.

Eight individuals with biallelic pathogenic variants in *KIAA0753* had been previously described in the medical literature, only one of which presented prenatally. In contrast, all 4 of the patients we describe presented with abnormalities detected during pregnancy. While this may in part be attributable to improved diagnostic imaging, we propose it may be related to more severe presentations of our patients. Given similar degree of non-rescue among the 6 variant proteins we studied *in vitro*, we speculate that suggests that genetic or environmental modifiers may underlie phenotypic heterogeneity in these patients.

Our RNAseq analysis of patient versus control fibroblasts suggests that pathogenic variants in *KIAA0753* result in an abnormal signal transduction of both Shh and Wnt pathways. Shh signaling is a major contributor to early embryo development; it controls neuroepithelial patterning and CNS development including axon guidance and neuronal activity (13, 14). The primary cilium is required for Shh signaling and deletion or mutation of genes which disrupt Shh signaling via loss of ciliogenesis result in a wide range of deficits in neural stem cells, neural patterning, hippocampal neurogenesis, and cerebellum development (15). Similarly, the Wnt signaling pathway affects many aspects of development including cell fate determination, organogenesis, cell migration and polarity, and neural patterning (14, 16, 17). It is well-established that defects in primary cilia or the basal body cause aberrant activation and general disruption of canonical and noncanonical Wnt signaling, respectively (18, 19). Interestingly, Abdelhamad et al. showed that mutations in *TMEM67* can cause either Joubert Syndrome or Meckel-Gruber syndrome; while mice with either disease manifestation show diminished Shh signaling, Joubert-like mice also exhibit downregulated canonical Wnt signaling and a slight increase in noncanonical Wnt (20). In this study, we show that Shh signaling is downregulated/disrupted in both immortalized and *KIAA0753* patient fibroblasts. Additionally, RNAseq data from *KIAA0753* patient cells suggests a defect in some aspects of Wnt signaling.

In conclusion, we have described 4 new individuals with bialellic pathogenic variants in *KIAA0753* whose phenotypes highlight some of the more severe phenotypes on the ciliopathy spectrum. Our *in vitro* assessment of the variants was consistent with pathogenic effects on ciliogenesis, but with no apparent genotype-phenotype correlation. Finally, our RNAseq data demonstrate disruption of both Shh and Wnt signaling may underlie the pathogenesis of *KIAA0753*-related ciliopathy phenotypes.

Methods

Patient Identification

Patients 1 and 2 were enrolled in a gene discovery research protocol (CCHMC IRB 2014-3789, PI RWS). Biallelic *KIAA0753* variants were identified during research re-analysis of patient 1's clinical trio exome and confirmed in patient 1 and his brother (patient 2) via targeted clinical Sanger sequencing. A skin biopsy was performed on patient 1 and fibroblasts were cultured as described below.

Patient 3 was diagnosed via clinical exome trio and Patient 4 was identified via research panel testing as described by Bachman—Gagescu et al (2015) (21). Written consent for publication was obtained from the families of patients 3 and 4.

Cell culture

Fibroblasts from control human fibroblasts, patient 1, and NIH3T3 fibroblasts were cultured in Dulbecco Modified Eagle Medium supplemented with 10% fetal bovine serum (FBS) and 1% penicillin/streptomycin at 37°C and 5% CO2. Cells were enzymatically detached from plates using 1 mL trypsin/EDTA (0.25%).

Plasmid transfection

We purchased FLAG-tagged plasmids containing the wild-type human KIAA0753 sequence and each of 6 patient variants, which were made by site-directed mutagenesis (Genscript). Plasmids were confirmed to have the correct insert via validation of Sanger sequencing provided by Genscript. Plasmids were transformed into TOP10 competent cells and grown on an LB-Agar coated plate with Kanamycin antibiotic (50μM) at 37°C overnight. Individual colonies were grown in liquid culture and plasmid DNA was isolated using a QIAGEN Plasmid Midi Kit. Plasmid DNA was then transfected into NIH3T3 cells at 70% confluency with Lipofectamine 3000 following the vendor protocol. Transfection efficiency was assessed after 48 hours by visualizing fluorescence of a control GFP plasmid(22). Plasmids are listed in Supplementary Table 1.

CRISPR/Cas9 transfection

CRISPR guides were designed using the Benchling online tool (benchling.com), which screens candidate guides for on-target efficiency and off-target effects. These guides were ligated into the PX459 entry plasmid (pSpCas9(BB)-2A-Puro (PX459) V2.0)(23). Plasmid was transfected for 48 hours as described above. Cells were then treated with puromycin for 72 hours. After a 48 hour recovery, cells were serially diluted into a 96-well plate (Corning protocol, 4000 cells/plate) for clonal dilution. Wells with only a single colony were grown to confluency, passaged into 6-well plates, and DNA was extracted for PCR to confirm CRISPR editing of the KIAA0753 locus. PCR product was purified with a DNA Clean & Concentrator kit (Zymo Research) and Sanger sequenced (Supplementary Data Figure). CRISPR guides and primers for genotyping are in Supplementary Table 2.

Western blotting

For protein extraction, RIPA buffer containing 1:100 protease and phosphatase inhibitor was added to the cells, then lysate was incubated at 4°C for 30 mins prior to centrifugation for 15 mins. Supernatant was harvested and stored at −80°C. Protein concentration was quantified using BCA assay. Blotting: 30 ug of protein was diluted 1:1 in 50:1 Laemmli buffer: B-mercaptoethanol and boiled at 95°C for 5 minutes. 8% gels were run at 130V for 90 mins. Protein was transferred to an Immobilon-FL membrane in Tris-Glycine buffer. Membranes were blocked in Intercept buffer (Licor) for 1 hour, then incubated in primary antibody diluted in Intercept buffer overnight at 4°C and secondary antibody (1:15000)

for 1 hour. Membranes were imaged on a Licor instrument and quantified. Antibodies and concentrations are listed in Supplementary Table 3.

Immunocytochemistry

Cells were plated onto coverslips in a 24-well tissue culture plate. They were serum-starved in Opti-MEM Reduced-Serum Medium for 24 hours prior to fixation in 4% paraformaldehyde. To permeabilize cell membranes, coverslips were immersed in 0.1% Triton-X 100 for 5 minutes prior to blocking. Coverslips were blocked in 4% NGS for 30 mins before addition of primary antibodi(es) at 4°C overnight. Secondary antibody was applied for 1 hour, then coverslips were co-stained with DAPI for 15 min. They were sealed to glass slides with ProLong Gold Antifade Mountant. Images were acquired on a Nikon C2 Confocal Microscope. Antibodies and concentrations for immunocytochemistry are listed in Supplementary Table 3.

For analysis of primary ciliation after plasmid transfection, immunocytochemistry slides were blinded to the experimentalist. Z-stack images were then taken on a Nikon C2 Confocal Microscope at 60x magnification. Cilia were quantified by hand-counting these images, with 70-130 cells per replicate per condition depending on the confluency of cells in each image. The transfection experiment and cell counting were repeated (n=2 or n=3) for each condition.

Quantitative Real-time Polymerase Chain Reaction (RT-qPCR)

Total RNA was extracted from cultured skin fibroblasts using the Trizol (Tri Reagent, Sigma Aldritch) protocol. 5 ug of RNA was reverse transcribed in a total reaction volume of 20 μL with the Superscript III First-Strand Synthesis System (Invitrogen). Real-time qPCR was performed using TaqMan Master Mix (Thermofisher). Primers for RT-qPCR analysis are listed in Supplementary Table 4.

RNA Sequencing

Human primary fibroblasts from an established control line and Patient 1 were grown in 6-well plates to 80% confluency. They were then serum starved for 24 hours and treated for 12 hrs with either Smoothened Agonist (SAG; 400nM), WNT3A conditioned media (cells from ATCC; media prepared in-house according to vendor protocol), or control media. RNA was extracted using the Trizol protocol as described above. RNA sequencing was performed by Novogene USA using standard protocols.

Supplementary Material

Refer to Web version on PubMed Central for supplementary material.

Acknowledgements

The authors are grateful to the patients and their families for participating in this project. Funding for this work is from the Cincinnati Children’s Research Foundation (R.W.S.) and NIH (R35GM121875 R.W.S.).

References

1. Elliott KH and Brugmann SA (2019) Sending mixed signals: Cilia-dependent signaling during development and disease. Dev Biol, 447, 28–41. [PubMed: 29548942]
2. Parisi MA (2019) The molecular genetics of Joubert syndrome and related ciliopathies: The challenges of genetic and phenotypic heterogeneity. Transl Sci Rare Dis, 4, 25–49. [PubMed: 31763177]
3. Chevrier V, Bruel AL, Van Dam TJ, Franco B, Lo Scalzo M, Lembo F, Audebert S, Baudelet E, Isnardon D, Bole A et al. (2016) OFIP/KIAA0753 forms a complex with OFD1 and FOR20 at pericentriolar satellites and centrosomes and is mutated in one individual with oral-facial-digital syndrome. Hum Mol Genet, 25, 497–513. [PubMed: 26643951]
4. Kodani A, Yu TW, Johnson JR, Jayaraman D, Johnson TL, Al-Gazali L, Sztriha L, Partlow JN, Kim H, Krup AL et al. (2015) Centriolar satellites assemble centrosomal microcephaly proteins to recruit CDK2 and promote centriole duplication. Elife, 4.
5. Faudi E, Brischoux-Boucher E, Huber C, Dabudyk T, Lenoir M, Baujat G, Michot C, Van Maldergem L, Cormier-Daire V and Piard J (2020) A new case of KIAA0753-related variant of Jeune asphyxiating thoracic dystrophy. Eur J Med Genet, 63, 103823. [PubMed: 31816441]
6. Vilboux T, Doherty DA, Glass IA, Parisi MA, Phelps IG, Cullinane AR, Zein W, Brooks BP, Heller T, Soldatos A et al. (2017) Molecular genetic findings and clinical correlations in 100 patients with Joubert syndrome and related disorders prospectively evaluated at a single center. Genet Med, 19, 875–882. [PubMed: 28125082]
7. Stephen J, Vilboux T, Mian L, Kuptanon C, Sinclair CM, Yildirimli D, Maynard DM, Bryant J, Fischer R, Vemulapalli M et al. (2017) Mutations in KIAA0753 cause Joubert syndrome associated with growth hormone deficiency. Hum Genet, 136, 399–408. [PubMed: 28220259]
8. Hammarsjo A, Wang Z, Vaz R, Taylan F, Sedghi M, Girisha KM, Chitayat D, Neethukrishna K, Shannon P, Godoy R et al. (2017) Novel KIAA0753 mutations extend the phenotype of skeletal ciliopathies. Sci Rep, 7, 15585. [PubMed: 29138412]
9. Romio L, Fry AM, Winyard PJ, Malcolm S, Woolf AS and Feather SA (2004) OFD1 is a centrosomal/basal body protein expressed during mesenchymal-epithelial transition in human nephrogenesis. J Am Soc Nephrol, 15, 2556–2568. [PubMed: 15466260]
10. Singla V, Romaguera-Ros M, Garcia-Verdugo JM and Reiter JF (2010) Ofd1, a human disease gene, regulates the length and distal structure of centrioles. Dev Cell, 18, 410–424. [PubMed: 20230748]
11. Aubusson-Fleury A, Lemullois M, de Loubresse NG, Laligne C, Cohen J, Rosnet O, Jerka-Dziadosz M, Beisson J and Koll F (2012) The conserved centrosomal protein FOR20 is required for assembly of the transition zone and basal body docking at the cell surface. J Cell Sci, 125, 4395–4404. [PubMed: 22718349]
12. Anvarian Z, Mykytyn K, Mukhopadhyay S, Pedersen LB and Christensen ST (2019) Cellular signalling by primary cilia in development, organ function and disease. Nat Rev Nephrol, 15, 199–219. [PubMed: 30733609]
13. Bisgrove BW and Yost HJ (2006) The roles of cilia in developmental disorders and disease. Development, 133, 4131–4143. [PubMed: 17021045]
14. Park SM, Jang HJ and Lee JH (2019) Roles of Primary Cilia in the Developing Brain. Front Cell Neurosci, 13, 218. [PubMed: 31139054]
15. Hoover AN, Wynkoop A, Zeng H, Jia J, Niswander LA and Liu A (2008) C2cd3 is required for cilia formation and Hedgehog signaling in mouse. Development, 135, 4049–4058. [PubMed: 19004860]
16. Gerdes JM and Katsanis N (2008) Ciliary function and Wnt signal modulation. Curr Top Dev Biol, 85, 175–195. [PubMed: 19147006]
17. May-Simera HL and Kelley MW (2012) Cilia, Wnt signaling, and the cytoskeleton. Cilia, 1, 7. [PubMed: 23351924]
18. Corbit KC, Shyer AE, Dowdle WE, Gaulden J, Singla V, Chen MH, Chuang PT and Reiter JF (2008) Kif3a constrains beta-catenin-dependent Wnt signalling through dual ciliary and non-ciliary mechanisms. Nat Cell Biol, 10, 70–76. [PubMed: 18084282]

19. Gerdes JM, Liu Y, Zaghloul NA, Leitch CC, Lawson SS, Kato M, Beachy PA, Beales PL, DeMartino GN, Fisher S et al. (2007) Disruption of the basal body compromises proteasomal function and perturbs intracellular Wnt response. Nat Genet, 39, 1350–1360. [PubMed: 17906624]

20. Abdelhamed ZA, Wheway G, Szymanska K, Natarajan S, Toomes C, Inglehearn C and Johnson CA (2013) Variable expressivity of ciliopathy neurological phenotypes that encompass Meckel-Gruber syndrome and Joubert syndrome is caused by complex de-regulated ciliogenesis, Shh and Wnt signalling defects. Hum Mol Genet, 22, 1358–1372. [PubMed: 23283079]

21. Bachmann-Gagescu R, Dempsey JC, Phelps IG, O'Roak BJ, Knutzen DM, Rue TC, Ishak GE, Isabella CR, Gorden N, Adkins J et al. (2015) Joubert syndrome: a model for untangling recessive disorders with extreme genetic heterogeneity. J Med Genet, 52, 514–522. [PubMed: 26092869]

22. Okuno T, Yamabayashi H and Kogure K (2010) Comparison of intracellular localization of Nubp1 and Nubp2 using GFP fusion proteins. Mol Biol Rep, 37, 1165–1168. [PubMed: 19263241]

23. Ran FA, Hsu PD, Wright J, Agarwala V, Scott DA and Zhang F (2013) Genome engineering using the CRISPR-Cas9 system. Nat Protoc, 8, 2281–2308. [PubMed: 24157548]

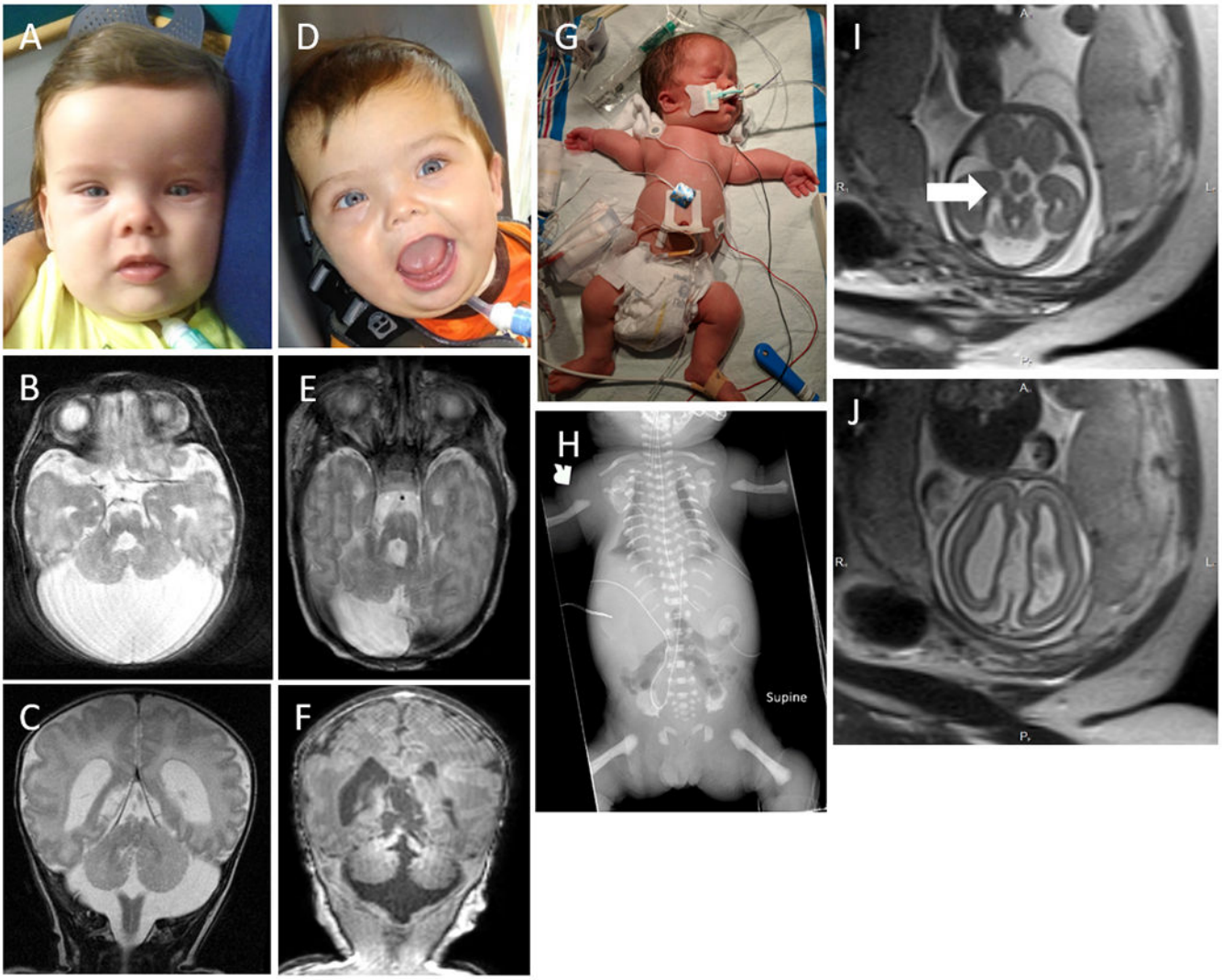

Figure 1: Photos and imaging of patients 1-4.

A-C, Patient 1. D-F, Patient 2. G-H, Patient 3. I-J, Patient 4. A and D demonstrate hypertelorism and frontal bossing; B,E,C, and F demonstrate cerebellar hypoplasia and molar tooth sign; H,I demonstrate short long bones and short ribs; J,K are fetal MRI images molar tooth sign (J) and ventriculomegaly (K).

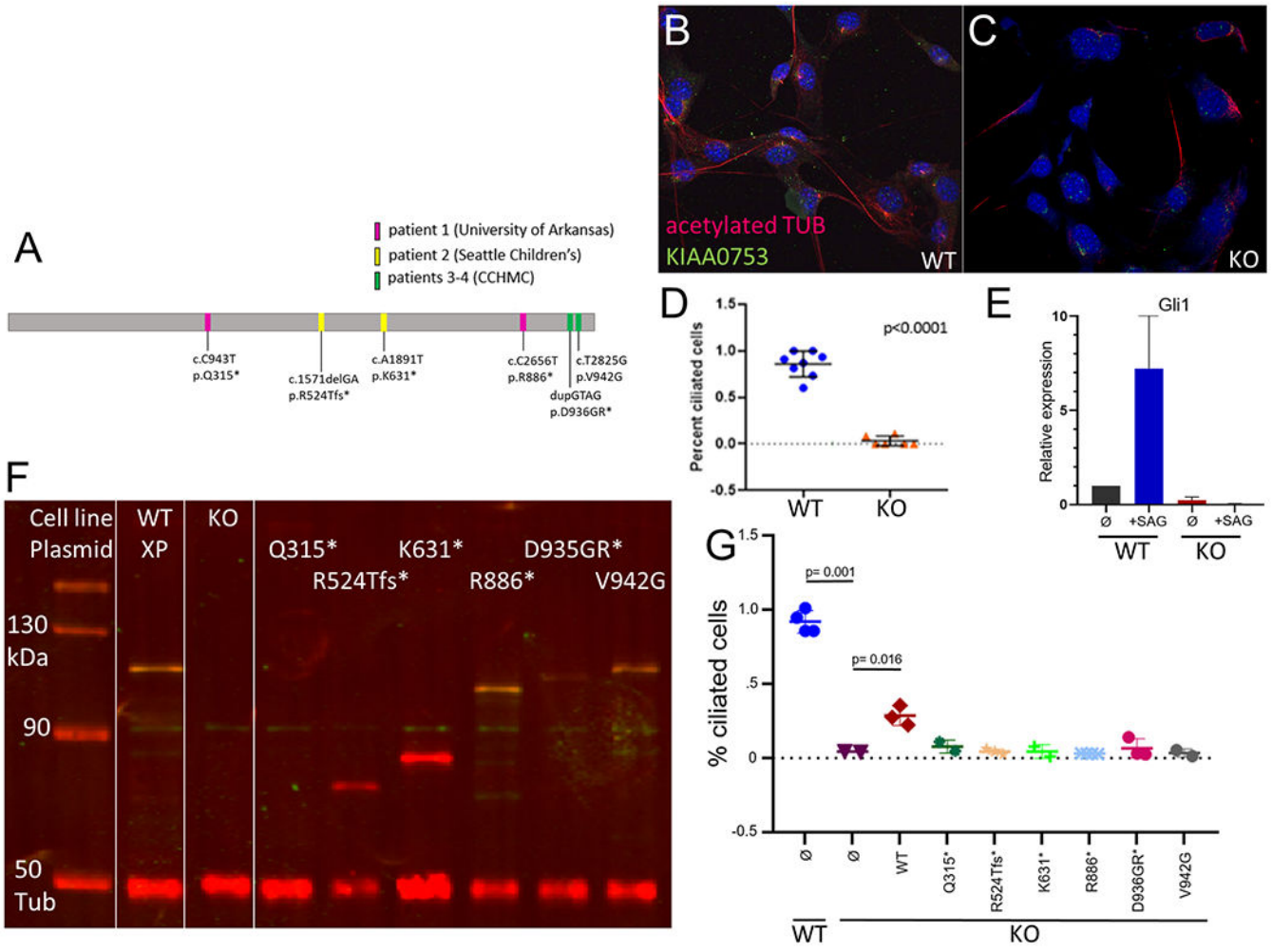

Figure 2: Deletion or mutation of KIAA0753 *in vitro* completely ablates primary ciliogenesis and *Shh* signaling.

A: CRISPR-Cas9-mediated targeting of KIAA0753 resulted in mutations at exon 3 leading to a large deletion in both alleles. B-C: NIH3T3 wild-type [WT] and KIAA0753 knock-out [KO] cells co-stained with acetylated tubulin, KIAA0753, and DAPI. D: Quantification of the complete loss of primary cilia in the KO line. E: qPCR for Gli1 of SAG-treated cells, indicating no response to *Shh* pathway stimulation in KO cells (n=3, GAPDH control). F: Western blots showing the relative protein sizes of KIAA0753 when NIH3T3 cells are transfected with either a wild-type plasmid (XP) or a plasmid containing each of six patient variants; Tubulin control and FLAG shown in red, KIAA0753 in green. G: Quantification of primary ciliation from immunocytochemistry, showing that wild-type KIAA0753 plasmid is capable of improving ciliogenesis whereas patient variant plasmids fail to do so (n=2 or n=3 for each condition).

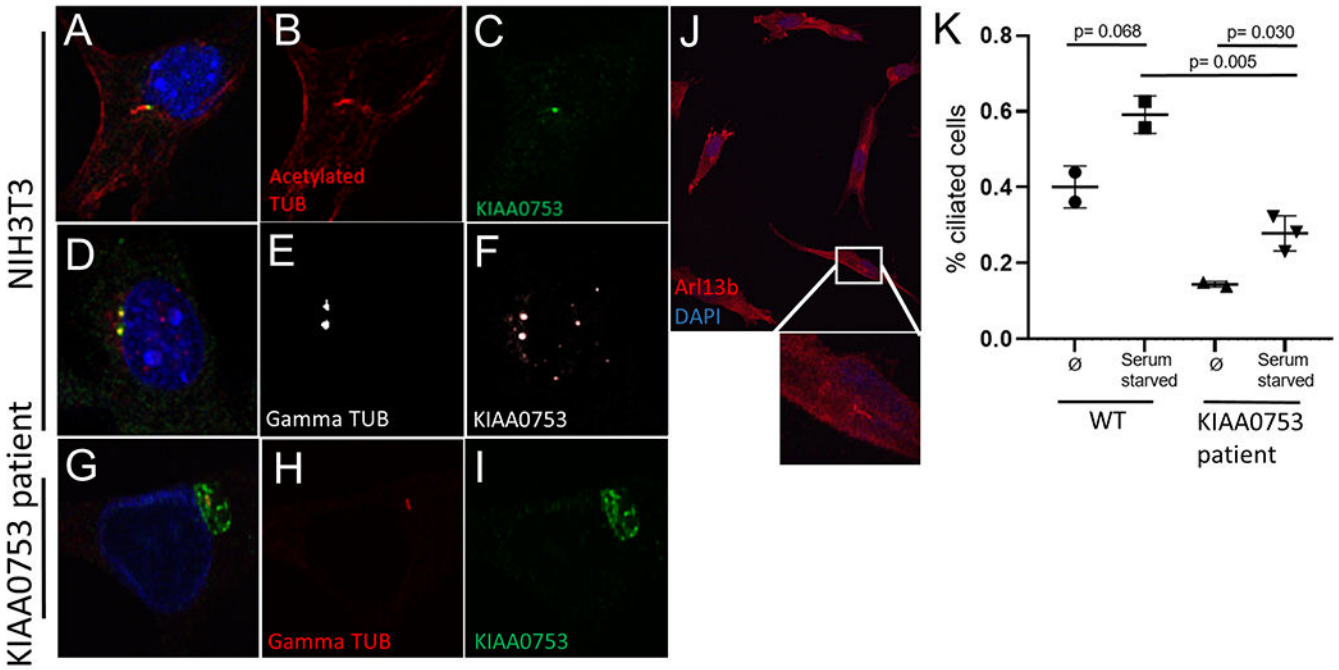

Figure 3: Patient fibroblasts exhibit decreased ciliogenesis.

(A-F) Subcellular localization of KIAA0753 in NIH3T3 cells co-stained with DAPI and acetylated tubulin (A-C) or gamma tubulin (D-F) [white is pseudo-colored]. G-I: Fibroblasts from one CCHMC KIAA0753 patient co-stained with gamma tubulin and KIAA0753. J: Patient fibroblasts with primary cilia visualized with Arl13b (J', inset of J). K: Quantification of number of ciliated cells in control vs patient fibroblast line.

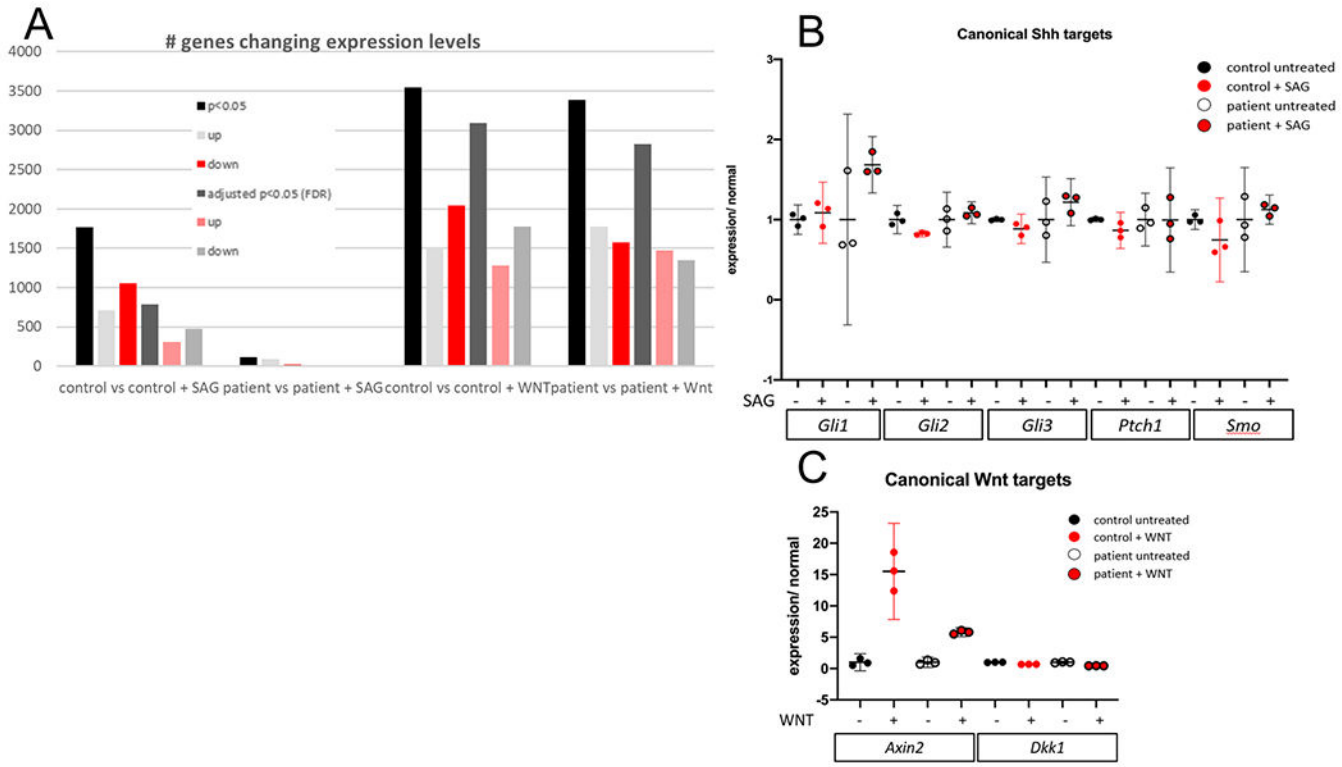

Figure 4: Patient fibroblasts show blunted *Shh* and *Wnt* signaling.

(A,B) RNA sequencing results show that patient fibroblasts have a generally blunted response to SAG stimulation (A) and correlating lack of expression change in *Shh* genes (B) and (C) do not upregulate *Axin2* in response to WNT3a treatment.

Table 1:

d phenotypes of 12 individuals with biallelic variants in *KIAA0753*

	Faudi	Stephen		Chevrier	Hammarsjö				This report	This report	This report	This report
	Patient 1	Patient 1	Patient 2	Patient 1	Patient 1	Patient 2	Patient 3	Patient 4	Patient 1	Patient 2	Patient 3	Patient 4
	c.943C>T/ c.943C>T	c.769A>G c.2359-1G>C		c.1891A>T c.1546-3C>A	c.970C>T c.970C>T			c.943C>T c.1271del	c.2803_2806dup c.2825T>G		c.943C>T c.2656C>T	c.1891A>T c.1571_1572delGA
	Q315* Q315*	R257G K787_Q789del		K631* D439Gfs*5	R324* R324*			Q315* P424Hfs*9	D936fs*3 V942G		Q315* R886*	K631* R524Tfs*7
	M	M	F	F	F	F	M	M	M	M	M	
ers	3300 g (−0.4), 50 cm (−1 SD) 39 cm (+4 SD)	Normal	Normal	Normal	Normal	Normal	Normal	Normal	Macrocephaly	Normal	Macrocephaly	
n	4 years	10 months	2 months	Birth	20 months	24 months	6 years	Prenatal	Prenatal	Prenatal	Prenatal	Prenatal
t n	narrow thorax, short limbs, severe respiratory and feeding diff from birth	Global developmental delay, hypotonia	Poor tracking and social skills	Facial dysmorphism, lobulated tongue, respiratory difficulties	Short stature, facial dysmorphism, skeletal anomalies	Short stature, skeletal anomalies	Respiratory difficulties, short stature, skeletal anomalies	Multiple anomalies led to termination	Apnea	Apnea	Respiratory failure, skeletal anomalies	Multiple anomalies led to termination
	Yes	N/A	N/A	N/A	Yes	Yes	Yes	Yes	No	No	Yes	No
es	Prominent forehead with hypertrichosis, depressed nasal bridge, anteverted nostrils, long philtrum, widely spaced teeth, large mouth	Frontal prominence, posteriorly rotated ears, bilateral epicanthal folds and down-turned corners of the mouth	Frontal bossing , bilateral epicanthal folds, and posteriorly rotated and borderline low-set ears	Flat facial profile, hypertelorism, wide nasal bridge with upturned nares, posteriorly low-set left ear	Frontal bossing, flat face, depressed nasal bridge, low-set ears	Frontal bossing, flat face, depressed nasal bridge	Frontal bossing, flat face, depressed nasal bridge, low-set ears	High forehead, frontal bossing, micrognathia, low-set ear, small nose, broad nasal bridge, long philtrum	Frontal bossing, flat nasal bridge, hypertelorism, short upturned nose	Frontal bossing, flat nasal bridge, hypertelorism, short upturned nose	Frontal bossing, low-set ears, anteverted nares	N/A
es	Narrowing of the occipitocervical juntion and cervical spinal cord without compression, mildly enlarged lateral ventricles, small posterior	Molar tooth sign, vermis dysplasia, ectopic pituitary	Molar tooth sign, vermis dysplasia, ectopic pituitary	Molar tooth sign, agenesis of corpus callosum, vermis hypoplasia, ventricular dilatation	Molar tooth sign, hypoplastic corpus callosum, small pituitary gland, inferior vermis dysplasia, dilated third	Molar tooth sign, hypoplastic corpus callosum, small pituitary gland, inferior vermis hypoplasia, dilated lateral ventricles	None	Ventriculomegaly, vermis dysplasia	Molar tooth sign, dysgenic corpus callosum, ventriculomegaly, vermis hypoplasia, large posterior fossa cyst, polymicrogyria	Molar tooh sign, vermis hypoplasia, polymicrogyria	Ventriculomegaly, vermis hypoplasia	Ventriculomegaly, agenesis of the corpus callosum, vermis dysplasia, small defect in the foramen magnum at the base of the skull

	Faudi	Stephen		Chevrier	Hammarsjö				This report	This report	This report	This report
	left cerebellum arachnoid cyst				ventricle ventricle							
nent	Global delay	Global developmental delay, hypotonia	Global developmental delay, hypotonia	N/A	Delayed motor development, Intellectual disability, hypotonia	Gross motor and speech delay	Gross motor and speech delay	N/A	Hypotonia, global delay, trach and vent dependent, g-tube	Hypotonia, global delay, trach and vent dependent, g-tube	N/A	N/A
	short stature (height −5.5 SD, 77 cm, at age 4)	Growth retardation and growth hormone deficiency	Growth retardation and growth hormone deficiency	N/A	Short stature	Short stature	Short stature	Short stature	Macrocephaly	Macrocephaly	Macrocephaly	Head circumference 2 weeks ahead prenatally
	moderate hepatomegaly	None	None	N/A	None	None	Mild hepatomegaly	None	None	None	N/A	None
	normal	None	None	Hydronephrosis	None	None	None	Mild pelviectasis	None	None	None	None
		Oculomotor apraxia	Hyperopia and esotropia, oculomotor apraxia	N/A	N/A	N/A	Normal	Normal	N/A	Normal	N/A	N/A
lies		None	None	Postaxial polydactyly, hallux duplication	Genu varum, narrow thorax, pectus excavatum, rhizomelia, contractures, brachydactyly	Genu varum, brachydactyly, contractures	Pectus carinatum, narrow chest, short limbs, brachydactyly	Short limbs, narrow chest, brachydactyly	Bilateral postaxial polydactyly	normal	Short limbs, narrow chest, brachydactyly	Unilateral polydactyly
s	trident appearance of pelvis and acetabular spurs, short limbs, narrow thorax, coronal cleft in Th5-6-8-12 vertebrae, diffuse osteosclerosis, brachydactyly, irrregular talus/ calcaneus ossification	N/A	N/A	N/A	Short ribs, trident ilia, broad metaphyses, short and bowed tubular bones, short metacarpals, cone-shaped epiphyses	Short ribs, trident ilia, broad metaphyses, short and bowed tubular bones, short metacarpals, cone-shaped epiphyses	Short ribs, trident ilia, broad metaphyses, short and bowed tubular bones, short metacarpals, cone-shaped epiphyses	Short ribs, trident ilia, broad metaphyses, short and bowed tubular bones, short metacarpals	Normal hip chest x-rays	N/A	Short ribs, trident ilia, broad metaphyses, short and bowed tubular bones, short metacarpals	N/A
	feeding tube and tracheostomy at 2 months, Trach out at 21	N/A	N/A	lobulated tongue, clefting of the alveolar ridges	Teeth hypoplasia, neonatal seizures	Teeth hypoplasia, neonatal seizures	Pulmonary hypertension. Died from respiratory	Micropenis, hypospadias	Trach and vent dependent, GJ tube feeding	Urachal cyst, bilateral inguinal hernias	Hypospadias, cryptorchidism. Severe RV hypertension.Died at 2 weeks	N/A

	Faudi	Stephen		Chevrier	Hammarsjö				This report	This report	This report
	months. Prenatal short femurs and polyhydramnios (third trimester)							failure at age 7 years			
Jeune syndrome	JTBS	JTBS		OFDVI	Skeletal ciliopathy + JTBS	Skeletal ciliopathy + JTBS	SRPS	Skeletal ciliopathy + JTBS	JTBS	SRPS	MKS+JTBS

ndrome; OFDVI, orofacial digital syndrome VI; SRTD, Short-rib ±polydactyly syndrome (SRPS),; MKS, Meckel syndrome